Effector-mediated subversion of proteasome activator (PA)28αβ enhances lysosomal targeting of *Legionella pneumophila* within cytokine-activated macrophages

Tshegofatso Ngwaga[1], Deepika Chauhan[1], Abigail G. Salberg[1], and Stephanie R. Shames[1]*

Division of Biology, Kansas State University, Manhattan, Kansas, 66506

*Correspondence: sshames@ksu.edu; @shames_lab

Phone: (785) 532-0110

Address: 347 Ackert Hall, 1717 Claflin Road, Manhattan, Kansas, 66506 USA

Keywords: PA28, proteasome, phagolysosomal fusion, cytokines, cell-autonomous immunity, *Legionella pneumophila*, LegC4, proteostasis, oxidative stress

Abstract

Legionella pneumophila is a natural pathogen of protozoa that causes Legionnaires' Disease pneumonia via replication within host macrophages using an arsenal of hundreds of translocated virulence factors termed effector proteins. Effectors are critical for intracellular replication but can also enhance pathogen clearance by mammalian hosts via effector-triggered immunity. The effector LegC4 confers a fitness disadvantage on *L. pneumophila* in mouse models of Legionnaires' Disease and uniquely potentiates the antimicrobial activity of macrophages activated with either tumor necrosis factor (TNF) or interferon (IFN)-γ. Here, we investigated the mechanism by which LegC4 enhances macrophage restriction of *L. pneumophila* and found a central role for the induced proteasome activator (PA)28αβ. PA28αβ facilitates ubiquitin-independent proteasomal degradation of oxidant-damaged proteins to relieve oxidative stress and impaired proteasome activity results in compensatory upregulation of lysosomal degradation pathways. We found that LegC4 binds the conserved PA28α subunit and that the LegC4 restriction phenotype is abolished within PA28αβ-deficient macrophages. Moreover, LegC4 impaired the resolution of oxidative proteotoxic stress and enhanced cytokine-dependent phagolysosomal fusion with the *Legionella*-containing vacuole. PA28αβ has been traditionally associated with antigen presentation and adaptive immunity; however, our data support a model whereby suppression of PA28αβ by LegC4 culminates in the cell-autonomous lysosomal killing of *L. pneumophila* within activated macrophages. This work provides a solid foundation on which to evaluate induced proteasome regulators as mediators of innate immunity.

36 **Significance Statement**

37 Pro-inflammatory cytokines induce antimicrobial host defense pathways within macrophages to
38 control intracellular pathogens. We discovered that the *Legionella pneumophila* effector protein
39 LegC4 potentiates pathogen clearance within cytokine-activated macrophages. Here, we investi-
40 gated LegC4 function and found that host proteasome activator (PA)28αβ was required for
41 LegC4 restriction within macrophages. PA28αβ is cytokine-induced and facilitates proteasomal
42 degradation of oxidant-damaged proteins. We found that LegC4 binds PA28α and impairs the
43 resolution of oxidative stress. Loss of proteasome activity causes compensatory upregulation of
44 lysosomal degradation pathways and, concomitantly, LegC4 increases phagolysosomal fusion
45 with *Legionella*-containing vacuoles. These findings support a model whereby pathogen subver-
46 sion of host proteostasis machinery triggers lysosomal pathogen targeting within activated mac-
47 rophages.

48

Introduction

Many intracellular bacterial pathogens cause disease by replicating within host macrophages (1). Macrophages activated by T_H1 proinflammatory cytokines, such as tumor necrosis factor (TNF) and interferon (IFN)-γ, are potently and broadly microbicidal. However, activated macrophages are in a state of altered protein homeostasis (proteostasis), owing in part to robust production of reactive oxygen species (ROS), which cause collateral damage to cellular proteins. To cope with oxidative stress, cytokine signaling induces expression of proteasome activator (PA)28αβ, which engages proteolytic 20S proteasome core particles (CPs) and facilitates degradation of oxidant-damaged proteins (2). Impaired proteasome activity causes compensatory upregulation of lysosomal degradation pathways, which are central to cell-autonomous immunity within activated macrophages (3). PA28αβ has been traditionally associated with antigen presentation and adaptive immunity (4, 5); however, the contribution of PA28αβ and oxidative proteotoxic stress to antimicrobial host defense has not been investigated.

Legionella pneumophila is a natural pathogen of freshwater amoebae and the causative agent of Legionnaires' Disease pneumonia, which results from bacterial replication within alveolar macrophages. To establish its intracellular niche, the *Legionella*-containing vacuole (LCV), *L. pneumophila* employs hundreds of virulence factors, called effector proteins, that are translocated into infected host cells by a Dot/Icm type IV secretion system (T4SS) (6). Effectors are essential for virulence, but their activity can also trigger upregulation of pro-inflammatory cytokine production by infected macrophages via effector-triggered immunity (ETI) (7–9). We discovered that the *L. pneumophila* effector LegC4, which is a *bona fide* virulence factor in amoebae, confers a fitness disadvantage on *L. pneumophila* in a mouse model of Legionnaires' Disease (10). The *in vivo* LegC4 restriction phenotype is likely due to elevated levels of pro-inflammatory cytokines in the *L. pneumophila*-infected lung since LegC4 impairs *L. pneumophila* replication within cultured macrophages activated with either tumor necrosis factor (TNF) or interferon (IFN)-γ (10, 11).

75 LegC4 is the only *L. pneumophila* effector that confers quantifiable opposing host-dependent fit-
76 ness phenotypes and the specific augmentation of cytokine-mediated restriction represents a po-
77 tentially novel mechanism of ETI. However, the mechanism by which LegC4 functions and en-
78 hances cytokine-mediated restriction of *L. pneumophila* is unknown.
79
80 Here, we investigated how LegC4 activity suppresses *L. pneumophila* replication within activated
81 macrophages. We found that LegC4 interacts with host PA28α and that LegC4-mediated re-
82 striction was abolished within PA28αβ-deficient (*Psme1/2*$^{-/-}$) bone marrow-derived macro-
83 phages. We further revealed that LegC4 impairs resolution of oxidative proteotoxic stress, which
84 is sufficient to induce the LegC4 restriction phenotype, and that LegC4 induces phagolysosomal
85 fusion with intracellular *Legionella*-containing vacuoles (LCVs). In sum, these results support a
86 model whereby PA28αβ targeting by a translocated effector protein perturbs proteostasis and en-
87 hances lysosomal targeting and restriction of *L. pneumophila* within cytokine-activated macro-
88 phages.
89
90 **Results**
91 **LegC4 potentiates redundant cytokine-mediated restriction of *L. pneumophila*** We
92 previously reported that LegC4 confers a fitness disadvantage on *L. pneumophila* in intranasal
93 mouse models of Legionnaires' Disease (LD) and within cytokine-activated macrophages (10, 11).
94 C57Bl/6 mice are restrictive to *L. pneumophila* due to flagellin-mediated activation of the
95 NAIP5/NLRC4 inflammasome (12, 13). Thus, we leveraged a flagellin (FlaA)-deficient *L. pneu-*
96 *mophila* (Δ*flaA*), an established model used to study FlaA-independent host responses within
97 C57Bl/6 mouse models of infection (12, 13). Using competitive index experiments, we found that
98 *L. pneumophila* Δ*flaA*Δ*legC4* mutant strains outcompeted parental Δ*flaA* strains in the lungs of
99 C57Bl/6 wild-type (WT) mice (11). However, no LegC4 fitness phenotype was observed within
100 isogenic WT bone marrow-derived macrophages (BMDMs) (11). *L. pneumophila* replicates within

101 alveolar macrophages in the lung, but we did not observe any LegC4-dependent differences in *L.*
102 *pneumophila* replication within MH-S mouse alveolar macrophages (**Fig S1**). However, LegC4-
103 mediated restriction is observed within BMDMs activated with either purified recombinant
104 (r)TNF or rIFN-γ (11). Thus, the phenotype observed for LegC4 *in vivo* is likely due to enhanced
105 levels of cytokines seen in the *L. pneumophila*-infected lung compared to cultured macrophages
106 (14). Alternatively, a phenotype for LegC4 can be observed in non-cytokine activated (naïve)
107 BMDMs by overexpressing *legC4* from an inducible promoter on a complementing plasmid (**Fig**
108 **1A**) (11). The LegC4 restriction phenotype is not exclusive to mouse macrophages since LegC4
109 confers a comparable fitness disadvantage on *L. pneumophila* within human THP-1 macrophages
110 (**Fig 1B**). Further support and utility of the LegC4 overexpression model was evidenced by loss of
111 LegC4-mediated restriction within BMDMs unable to produce or respond to endogenous TNF
112 (*Myd88*$^{-/-}$ and *Tnfr1*$^{-/-}$, respectively) (**Fig 1C, 1D**) (11). IFN-γ signaling is sufficient for LegC4 re-
113 striction (11); however, the LegC4 restriction phenotype was retained within *Ifngr1*$^{-/-}$ BMDMs
114 (**Fig 1E**), indicating that the relatively low levels of IFN-γ secreted by macrophages are not nec-
115 essary for restriction. Furthermore, the loss of any single cytokine was not sufficient to restore *L.*
116 *pneumophila* fitness since LegC4 still conferred a fitness disadvantage on *L. pneumophila* within
117 the lungs of TNFR1-, MyD88- and IFNGR1-deficient mice (**Fig 1F**). These data further support
118 our previous work showing that LegC4 augments redundant cytokine-mediated pathogen re-
119 striction mechanisms (11). While overexpression of *legC4* is not necessary to observe a phenotype,
120 this infection model is robust and useful for our goal to define LegC4 function and mechanisms
121 of cytokine-mediated restriction within macrophages.
122
123 **LegC4 binds host proteasome activator (PA)28α**. To gain insight into the mechanism of
124 LegC4 function, we conducted a yeast two-hybrid (Y2H) interactomics screen using LegC4 as bait
125 and genomic (g)DNA from mouse splenocytes as prey. This screen revealed interactions between
126 LegC4 and several regulators of eukaryotic proteasomes, including proteasome activator (PA)

127 28α, PA28γ, and Ecm29 (**Table S1**). The highest-confidence interactor was PA28α with 28 indi-
128 vidual clones, all of which encoded a minimal overlapping region in the PA28α C-terminal domain
129 (amino acid residues 105-249) (**Table S1**, **Fig S2**). We initially evaluated the PA28α-LegC4 in-
130 teraction by reciprocal co-immunoprecipitation from lysates of HEK 293T cells ectopically pro-
131 ducing epitope-tagged PA28α and LegC4. We found that PA28α-Myc co-immunoprecipitated
132 with 3xFLAG-LegC4 and that 3xFLAG-LegC4 co-immunoprecipitated with GFP-PA28α (**Fig 2A**).
133 We also found that ectopically produced GFP-PA28α and 3xFLAG-LegC4 localize within trans-
134 fected HeLa cells (**Fig 2B**). Ectopic expression of PA28α was necessary since it is normally ex-
135 pressed only in response to cytokine signaling (15, 16). Together, these data suggest that LegC4
136 binds host PA28α, which has not been previously identified as a target of bacterial effectors and
137 provides an explanation as to why LegC4 only has a phenotype within cytokine-activated cells.
138
139 **PA28αβ contributes to LegC4-dependent and -independent macrophage restriction**
140 **of *L. pneumophila*.** Based on the interaction between PA28α and LegC4, we tested the hypoth-
141 esis that PA28α contributes to LegC4-mediated restriction of *L. pneumophila* within BMDMs.
142 PA28α-deficient (*Psme1*$^{-/-}$) mice are not commercially available, so we evaluated the role of
143 PA28α using BMDMs derived from PA28αβ-deficient (*Psme1/2*$^{-/-}$) mice. PA28α associates with
144 PA28β to form the PA28αβ (11S) proteasome regulator. PA28β is homologous to PA28α, but is
145 strictly dependent on PA28α for activity and is hypothesized to enhance the interaction of PA28α
146 with 20S proteolytic proteasome core particles (CPs) (17). We found that PA28αβ was necessary
147 for LegC4-mediated restriction of *L. pneumophila* since it was abolished within *Psme1/2*$^{-/-}$
148 BMDMs (**Fig 2C**). Moreover, replication of *L. pneumophila* Δ*flaA* was attenuated within naïve
149 and cytokine-activated *Psme1/2*$^{-/-}$ BMDMs (**Fig 2D**), which phenocopies LegC4 and supports the
150 hypothesis that LegC4 impairs PA28α activity. Since autocrine and paracrine TNF signaling is
151 sufficient for the LegC4 restriction phenotype, we tested whether PA28αβ or LegC4 enhance TNF

152 secretion from *L. pneumophila*-infected BMDMs. However, we found no LegC4- or PA28αβ-me-
153 diated differences in TNF secretion from infected BMDMs (**Fig S3**). We also found that viability
154 of *L. pneumophila*-infected BMDMs was unaffected by either LegC4, PA28αβ, or exogenous rTNF
155 compared to untreated cells (**Fig S4**). These data suggest that the LegC4 restriction phenotype is
156 dependent on PA28αβ and occurs independently of increased cytokine secretion or cell death,
157 which support a novel role for PA28αβ in cell-autonomous immunity against an intracellular bac-
158 terial pathogen.
159
160 **LegC4 impairs resolution of oxidative proteotoxic stress.** In cells of the innate immune
161 system, PA28α is produced in response to oxidative stress, TNF, or IFN-γ and forms a heterohep-
162 tameric complex with PA28β to assemble the 11S (PA28αβ) proteasome regulator (2, 16, 18, 19).
163 PA28αβ associates with proteasome CPs to generate antigenic peptides and resolve oxidative pro-
164 teotoxic stress by facilitating ubiquitin-and ATP-independent proteasomal degradation of oxi-
165 dant-damaged (carbonylated) proteins (4, 20). Since PA28αβ was required for LegC4-mediated
166 *L. pneumophila* restriction within BMDMs (see Fig 2C), we tested the hypothesis that LegC4 im-
167 pairs resolution of oxidative proteotoxic stress by quantifying protein carbonyls in cell lysates.
168 We directly evaluated how LegC4 impacts resolution of oxidative proteotoxic stress by
169 quantifying protein carbonyls within RAW 264.7 cells stably producing 3xFLAG-LegC4 (RAW-
170 LegC4). We confirmed production of 3xFLAG-LegC4 by confocal microscopy (**Fig 3A**) and West-
171 ern blot (**Fig 3B**). Immunoprecipitation of 3xFLAG-LegC4 was necessary due to its low abun-
172 dance. However, we validated that ectopically produced LegC4 was active, since replication of *L.*
173 *pneumophila* Δ*flaA* within RAW-LegC4 cells was attenuated compared to control (RAW-Cntrl)
174 cells (**Fig 3C**). To test the hypothesis that LegC4 impairs resolution of oxidative proteotoxic
175 stress, we quantified protein carbonyls using ELISA within lysates of RAW-LegC4 and -Cntrl cells
176 treated with hydrogen peroxide (H_2O_2). H_2O_2 is commonly used to induce oxidative stress since

177 superoxide radical ($O_2^{\cdot-}$) (precursor to H_2O_2) is unstable in solution (21–23). We found that the
178 concentration of protein carbonyls in lysates of H_2O_2-treated RAW-LegC4 cells was significantly
179 greater than control cells (**Fig 3D**) and that LegC4 alone did not affect the concentration of pro-
180 tein carbonyls in untreated cells (**Fig 3D**). These data suggest that LegC4 is sufficient to impair
181 resolution of oxidative proteotoxic stress.

182 We subsequently evaluated how LegC4 impacts the abundance of protein carbonyls within
183 *L. pneumophila*-infected cells. To control for LegC4-mediated differences in bacterial replication
184 within WT BMDMs, we leveraged *Tnfr1*$^{-/-}$ BMDMs (see Fig 1). *Tnfr1*$^{-/-}$ BMDMs were infected for
185 4 h in the presence or absence of H_2O_2 and protein carbonyls were visualized by Western blot. We
186 found that the abundance of protein carbonyls was increased within H_2O_2-treated BMDMs in-
187 fected with *L. pneumophila* Δ*flaA*Δ*legC4* (p*legC4*) relative to Δ*flaA* and empty vector control
188 strains (**Fig 3E**). Within untreated BMDMs, infection with the avirulent *dotA*::Tn strain increased
189 the abundance of protein carbonyls (**Fig 3E**), which is likely a consequence of increased global
190 ROS production by macrophages infected with avirulent compared to virulent *L. pneumophila*
191 (24). Since no LegC4-mediated differences were observed within untreated *Tnfr1*$^{-/-}$, it is unlikely
192 that the increase in protein carbonyls observed is due to a LegC4-mediated upregulation global
193 ROS production by infected BMDMs. Together, these data support our hypothesis that LegC4
194 impairs resolution of oxidative proteotoxic stress within macrophages.

195

196 **Oxidative stress is sufficient for LegC4-mediated restriction.** Based on our data showing
197 that LegC4 impairs resolution of oxidative proteotoxic stress, we hypothesized that oxidative
198 stress is sufficient for LegC4-mediated restriction within BMDMs. To test this hypothesis, we
199 quantified *L. pneumophila* replication within *Tnfr1*$^{-/-}$ BMDMs, in which LegC4 is not restrictive
200 (see Fig 1C), in the presence or absence of a sublethal concentration of H_2O_2 to induce oxidative
201 stress. We found that replication of *L. pneumophila* Δ*flaA*Δ*legC4* (p*legC4*) strain was significantly
202 attenuated within H_2O_2-treated *Tnfr1*$^{-/-}$ BMDMs compared to *L. pneumophila* Δ*flaA* and

203 Δ*flaA*Δ*legC4* empty vector (pEV) control strains (**Fig 3F**). These differences represent a 78% de-
204 crease in colony forming units (CFU), which is striking since experimental limitations necessi-
205 tated a low concentration (10 μM) of H_2O_2. It is unlikely that growth attenuation was due to direct
206 *L. pneumophila* killing by H_2O_2 since *L. pneumophila* has evolved multiple complimentary strat-
207 egies to protect against oxidative stress and can withstand up to 2 mM H_2O_2 *in vitro* (orders of
208 magnitude greater than intracellular concentrations) (22, 24–26). Thus, these data suggest that
209 oxidative stress is sufficient for the LegC4 restriction phenotype.
210
211 **LegC4 increases phagolysosomal fusion with *Legionella*-containing vacuoles.** Our
212 current data show that LegC4 functions through PA28αβ and confers a fitness disadvantage under
213 oxidative stress conditions. Impaired proteasome activity causes compensatory upregulation of
214 lysosomal degradation pathways to cope with proteotoxic stress (3, 27). Based on our data show-
215 ing that oxidative proteotoxic stress is sustained in LegC4-producing cells, we tested the hypoth-
216 esis that LegC4 increases lysosomal targeting of *L. pneumophila* within activated macrophages.
217 Virulent *L. pneumophila* establish a replicative *Legionella*-containing vacuole (LCV) by blocking
218 endocytic maturation of their phagosome (28, 29). However, avirulent (*dotA*::Tn) *L. pneumophila*
219 are unable to establish a replicative LCV and phagosomes rapidly undergo endocytic maturation,
220 as evidenced by localization of the lysosomal membrane marker LAMP1 to *L. pneumophila*-con-
221 taining phagosomes (28) (**Fig S5**). We initially tested the hypothesis that LegC4 increases LAMP1
222 localization to LCVs by immunofluorescence microscopy and blinded quantification of $LAMP1^+$
223 LCVs. As expected, there were significantly fewer $LAMP1^+$ LCVs harboring Δ*flaA* and empty vec-
224 tor control strains compared to the avirulent control (**Fig 4A**). There was a significant increase in
225 the percentage of $LAMP1^+$ LCVs harboring Δ*flaA*Δ*legC4* (p*legC4*) compared to Δ*flaA* and empty
226 vector control strains within both WT and *Tnfr1*$^{-/-}$ BMDMs (**Fig 4A**). However, within WT
227 BMDMs, LAMP1 localization to LCVs harboring Δ*flaA*Δ*legC4* (p*legC4*) did not differ significantly
228 from the avirulent *dotA*::Tn strain (**Fig 4A**), which was surprising since plasmid expression of

229 *legC4* did not impair biogenesis of a replicative LCV (≥5 bacteria/vacuole) compared to *L. pneu-*
230 *mophila* Δ*flaA* and Δ*flaA*Δ*legC4* (pEV) control strains (**Fig 4B**). As expected, the avirulent con-
231 trol strain was significantly attenuated for replicative LCV formation compared to the parental *L.*
232 *pneumophila* Δ*flaA* strain (***P*<0.01, **Fig 4B**). These data correlate with our CFU data showing
233 that that LegC4 restriction is observed after 24 h of infection within BMDMs (Fig 1A) and chal-
234 lenge the dogma that LAMP1 localization and *L. pneumophila* intracellular replication are mutu-
235 ally exclusive. Moreover, these data support our hypothesis that LegC4 enhances phagolysosomal
236 fusion with LCVs.

237 We subsequently tested the hypothesis that phagolysosomal fusion is important for
238 LegC4-mediated restriction by quantifying *L. pneumophila* replication within BMDMs treated
239 with Bafilomycin A1 (BAF). BAF is a pharmacological inhibitor of the H^+-type vacuolar (v)-ATPase
240 that blocks vacuolar acidification and impairs phagolysosomal fusion (30). Thus, we evaluated
241 the contribution of phagolysosomal fusion to the LegC4 restriction phenotype by quantifying *L.*
242 *pneumophila* replication within BAF-treated BMDMs. LCV acidification is important for late
243 stages of the *L. pneumophila* lifecycle (31); however, intracellular replication is minimally im-
244 pacted within BMDMs treated with a low concentration (12.5 nM) of BAF (32). We found that the
245 LegC4 restriction phenotype was abolished within BAF-treated BMDMs (**Fig 4C**), suggesting that
246 phagolysosomal fusion and lysosomal acidification are important for LegC4-mediated restriction.
247 Together, our data support a central role for phagolysosomal fusion and vacuolar acidification in
248 LegC4-mediated restriction of *L. pneumophila* within BMDMs.

249

250 **Discussion**

251 This study supports a novel role for proteasome activator (PA)28αβ in cell-autonomous host de-
252 fense against an intracellular pathogen. We found that the *L. pneumophila* effector LegC4 en-
253 hances restriction of *L. pneumophila* within macrophages activated with either TNF or IFN-γ in
254 a PA28αβ-dependent manner. Our results suggest a model whereby LegC4 impairs resolution of

255 oxidative proteotoxic stress and promotes lysosomal restriction of *L. pneumophila* by subverting
256 PA28αβ activity (**Fig S6**). This model is supported by our data showing that LegC4 binds PA28α,
257 PA28αβ is required for the effects of LegC4 on host cells, LegC4 impairs resolution of oxidative
258 proteotoxic stress, and the contribution of both oxidative stress and phagolysosomal fusion to
259 LegC4-mediated restriction of *L. pneumophila*. This work is the first describe a role for PA28αβ
260 in innate and cell-autonomous host defense.
261
262 *L. pneumophila* is an accidental pathogen of humans that rarely transmits between infected indi-
263 viduals. Thus, an evolutionary basis for the LegC4-PA28α interaction can be explained by LegC4
264 targeting the PA28α homolog in amoebae. Indeed, the natural host *A. castellanii*, in which LegC4
265 is a *bona fide* virulence factor (10), encodes a PA28α homolog (*Ac*PA28) that shares 34% identity
266 with PA28α. Sequence identity between PA28α and *Ac*PA28 is primarily in the C-terminal do-
267 main, which is important for engaging 20S CPs and was contained in all PA28α clones identified
268 in our yeast two-hybrid screen (Fig 2A; Table S1). These data together with our observation that
269 the LegC4 phenotype is recapitulated in PA28αβ-deficient macrophages have led us to speculate
270 that LegC4 binding prevents PA28-CP complex formation. While the function of *Ac*PA28 has not
271 been described, structural studies have shown that mammalian PA28α and evolutionary distant
272 PA28s are similar and all associate with proteolytic proteasome core particles, suggesting that it
273 likely also functions as a proteasome regulator (33, 34). The constitutive 26S proteasome system
274 is central to *L. pneumophila*'s virulence strategy and its integrity may be preserved by sequester-
275 ing PA28 from CPs. We are currently investigating the molecular mechanism by which LegC4
276 regulates PA28 activity within mammalian cells and amoebae and how this activity is advanta-
277 geous to *L. pneumophila* in the natural host.
278

279 We found that inducing oxidative stress with hydrogen peroxide (H_2O_2) was sufficient for the
280 LegC4 restriction phenotype. H_2O_2 is routinely used to induce oxidative stress in laboratory mod-
281 els since both superoxide ($O_2^{\bullet-}$) and hydroxyl ($OH^{\bullet}$) radicals are highly reactive and unstable in
282 solution. Interestingly, reactive oxygen species (ROS) are important for *L. pneumophila* re-
283 striction by neutrophils but play a negligible role in macrophages (24, 35, 36). This difference has
284 been attributed to suppression of global intracellular ROS production and NADPH oxidase
285 (NOX2) trafficking to the LCV by virulent *L. pneumophila* within macrophages (24, 35). Direct
286 oxidative killing of *L. pneumophila* within activated macrophages is unlikely since *L. pneumoph-*
287 *ila* has evolved multiple complimentary strategies to protect against oxidative stress and can with-
288 stand up to 2 mM H_2O_2 *in vitro* (orders of magnitude greater than intracellular concentrations)
289 (22, 24–26). Moreover, *Tnfr1*$^{-/-}$ BMDMs treated with H_2O_2 did not suppress replication of *L.*
290 *pneumophila* control strains compared to untreated BMDMs (see Fig 3F). This suggests that the
291 concentration of H_2O_2 used in our study is insufficient for direct *L. pneumophila* killing. Future
292 studies will reveal whether LegC4 or PA28αβ impact the abundance or source of ROS within *L.*
293 *pneumophila*-infected macrophages.
294
295 Phagolysosomal fusion and autophagy are cytoprotective under inflammatory conditions and
296 central to cytokine-mediated cell-autonomous pathogen restriction. Lysosomal pathogen re-
297 striction within IFN-γ-activated macrophages involves immunity-related GTPases (IRGs), which
298 localize to and facilitate lysosomal trafficking to pathogen-containing phagosomes (37). Although
299 IRGs may contribute to restriction of LegC4-producing *L. pneumophila* strains within IFN-γ-ac-
300 tivated macrophages (38), we found that IFNGR1 signaling is dispensable for LegC4 restriction
301 (Fig 1E), which suggests that IRGs are not central drivers of LegC4-mediated *L. pneumophila*
302 restriction. A role for TNFR1-mediated signaling in lysosomal pathogen restriction has not been
303 well established. Canonically, TNF signaling activates extrinsic cell death pathways; however,
304 TNFR1-mediated signaling induces lysosomal fusion with LCVs within 3 h of *L. pneumophila*

305 infection within primary mouse BMDMs, which is more rapid compared to BMDMs activated with
306 IFN-γ (36). The mechanism by which TNF signaling enhances phagolysosomal fusion with LCVs
307 is poorly understood; however, upregulation of autophagy genes is cytoprotective against TNF-
308 induced death in myeloid cells (39). Autophagy is also upregulated to prevent aberrant pyroptotic
309 cell death below a certain threshold of inflammasome agonist (40). The NLRC4 inflammasome is
310 dispensable for LegC4-mediated restriction (10, 11), but a role for the NLRP3 inflammasome is
311 possible since it is activated by proteotoxic stress (41). Inflammasome components and pro-in-
312 flammatory cytokines are selectively degraded below a threshold of agonist. We are currently eval-
313 uating the role of autophagy and the NLRP3 inflammasome in PA28αβ- and LegC4-mediated re-
314 striction of *L. pneumophila*.
315
316 Virulent *L. pneumophila* establish a replicative LCV by avoiding endosomal maturation of their
317 phagosome. The current dogma dictates that lysosomal fusion with LCVs at early time points dur-
318 ing infection (≤ 16 h) prevents *L. pneumophila* intracellular replication (31, 42). We found that
319 plasmid expression of *legC4* induced robust LAMP1 localization to LCVs within WT BMDMs, sim-
320 ilar to what is seen for an avirulent a Dot/Icm-deficient strain. Since we observed no attenuation
321 in replicative LCV formation or intracellular replication by CFU assay by 24 h post-infection, these
322 data suggest that *L. pneumophila* intracellular replication and LAMP1 localization to LCVs are
323 not mutually exclusive. It is tempting to speculate that *L. pneumophila* replication within a
324 LAMP1^{+} LCV may result from translocated effectors that block v-ATPase activity, such as SidK
325 (43–46). Interestingly, loss of TNFR1-mediated signaling did not fully abrogate LegC4-mediated
326 LAMP1 localization to LCVs. We think this may be a consequence of sustained oxidative stress
327 downstream of pattern recognition receptors. However, phagolysosomal fusion with LCVs is not
328 sufficient for LegC4 to impair replication within Tnfr1-/- BMDMs, further supporting our obser-
329 vation that LegC4 restriction occurs in a dose-dependent manner. The properties of a replication

330 permissive LAMP1$^+$ LCV, the contribution of additional translocated effectors, and the contribu-
331 tion of canonical autophagic degradation pathways are currently being investigated in our lab.
332
333 In summary, we have uncovered a new role for PA28αβ and oxidative proteotoxic stress in cell-
334 autonomous pathogen restriction. This work is also the first to show bacterial pathogen targeting
335 of PA28α and suggests that suppression of PA28αβ activity may be a pathogen-triggered host
336 defense mechanism. Moreover, our data suggest that inhibition of PA28αβ may enhance innate
337 immunity against intracellular pathogens by potentiating existing inflammatory responses. Fu-
338 ture studies will provide further insight into the ubiquity and mechanism(s) of pathogen re-
339 striction induced by proteotoxic stress and suppression of PA28αβ activity.
340

341 **Materials & Methods**

342 Bacterial Strains, Plasmids, and Culture conditions

343 *Legionella pneumophila* strains used in this study (**Table S2**) were cultured on supplemented
344 charcoal N-(2-Acetamido)-2-aminoethanesulfonic acid (ACES)-buffered yeast extract (CYE) and
345 grown at 37˚C as described (47). Liquid cultures were grown overnight with shaking at 37˚C in
346 supplemented ACES-buffered yeast extract (AYE) medium, as described (11, 48). For plasmid
347 maintenance, CYE was supplemented with 10 μg mL^{-1} chloramphenicol and *legC4* expression was
348 induced with 1 mM isopropyl-β-D-1-thiogalactopyranoside (IPTG) where indicated. Plasmids
349 used in this study are listed in **Table S3**. Oligonucleotide primers are listed in **Table S4.**
350

351 Mice and bone marrow-derived macrophages

352 All mice were on a C57BL/6 background and purchased from the Jackson Laboratories (Bar Har-
353 bor, Maine) and in-house colonies were maintained in specific pathogen-free conditions at Kansas
354 State University. All experiments involving animals were approved by the Kansas State University

355 Institutional Animal Care and Use Committee (Protocols 4022, 4501, and 4386) and performed
356 in compliance with the Animal Welfare Act and NIH guidelines.
357 Bone marrow was harvested from seven- to twelve-week-old mice as described (49).
358 BMDMs were generated by differentiation in RPMI supplemented with 20% heat-inactivated fetal
359 bovine serum (HI-FBS) (Biowest, Riverside, MO) and 15% L929 cell supernatant for 6 days prior
360 to seeding for infection.
361
362 Competitive Index
363 Six- to twelve-week-old sex- and age-matched mice were infected as previously described. Mixed
364 bacterial inoculums (1:1) containing a total of 5 x 10^6 bacteria were diluted and plated on selective
365 medium (10 µg mL^{-1} chloramphenicol for plasmid selection). At 48 h post-infection, mice were
366 euthanized, and lung homogenates were plated on selective media as described (11). CFU were
367 enumerated and used to calculate CI values [$(CFUcm^R_{48h}/CFUwt_{48h})/(CFUcm^R_{IN})/CFUwt_{IN})$].
368
369 Molecular Cloning
370 Plasmids were generated for stable and transient ectopic production in mammalian cells. For pro-
371 duction of 3xFLAG-LegC4, *legC4* was amplified from *L. pneumophila* genomic (g)DNA using
372 LegC4BamHI-F/LegC4NotI-R primer pairs and cloned as a BamHI/NotI fragment into 3xFLAG
373 4/TO (50). To produce GFP-PA28α, *psme1* was amplified from pCMV-3Tag-4a::*psme1* (pur-
374 chased from Genscript, Piscataway, New Jersey) using Psme1Sal1-F/Psme1BamHI-R primer
375 pairs and cloned as a Sal1/BamH1 fragment into pEGFPC1 (Clontech). Plasmid DNA was trans-
376 fected into mammalian cells as described below.
377
378 Cell Culture and Transfections
379 HEK 293T, HeLa cells, RAW 264.7 cells, and MH-S cells (gifts from Dr. Craig Roy, Yale Univer-
380 sity) were maintained at 37˚C and 5% CO_2 in Dulbecco's Modified Eagle Medium (DMEM)

381 supplemented with 10% HI-FBS. THP-1 cells were maintained in RPMI supplemented with 10%
382 HIFBS and differentiated with 100 nM phorbal 12-myristate 13-acetate (PMA) for 4 days prior to
383 infection with *L. pneumophila* (see below). All cell lines were used between passage 4-20.
384 HEK 293T cells were transfected with purified plasmid DNA (**Table S2**) using calcium
385 phosphate as described (51). Lysates were generated from transfected cells after 48 h and used for
386 immunoprecipitation and Western blot analysis (see below). HeLa cells were seeded one day prior
387 to transfection with jetPRIME transfection reagent according to manufacturer's guidelines. Two
388 hours before transfection, HeLa cells were washed and incubated in low-serum media (DMEM
389 4% HIFBS. Media were replaced with DMEM 10% HIFBS four hours post-transfection and as-
390 sayed 24 h post-transfection.
391 To generate RAW 264.7 cells with stable plasmid integrations, cells were transfected with
392 pcDNA::*3xflag-legC4* or pcDNA::*3xflag* vector using a Nucleofector 2b electroporator (Lonza,
393 Basel, Switzerland) and cultured over 14 days with Zeocin selection for 14 days (200 -1000 μg mL^{-}
394 ^{1}). Stable RAW 264.7 cells were maintained in culture in the presence of 200 μg mL^{-1} Zeocin. For
395 *L. pneumophila* infections, cells were seeded one day prior to infection in the absence of Zeocin.
396
397 <u>Immunoprecipitation</u>
398 Transiently transfected HEK 293T cells or RAW 264.7 cells were washed with phosphate-buffered
399 saline and lysed in ice-cold NP-40 buffer [1% non-iodet P40 (v/v), 20 mM Tris pH 7.5, 150 mM
400 NaCl, 10 mM $Na_4P_2O_7$, 50 mM NaF, complete protease inhibitor (Roche)]. Lysates were clarified
401 and added to magnetic Protein G-conjugated Dynabeads that had been pre-incubated with either
402 mouse α-FLAG M2 antibody (Sigma Aldrich) or rabbit α-GFP antibody (Abcam, ab6556) accord-
403 ing to manufacturer's instructions. Input samples were collected from cell lysates prior to incuba-
404 tion with beads. Beads and input samples were resuspended in 3x Laemmli sample buffer for
405 Western blot analysis.
406

407 Western blot

408 Boiled protein samples were separated by SDS-PAGE and transferred to polyvinylidene difluoride
409 (PVDF) membrane using a BioRad TransBlot semidry transfer apparatus. Membranes were incu-
410 bated in blocking buffer [5% non-fat milk powder dissolved in Tris-buffered saline-0.1% Tween-
411 20 (TBST)]. Primary antibodies [rabbit a-FLAG (Sigma-Aldrich, F1804), rabbit a-Myc (Cell Sig-
412 naling, 2278S), rabbit a-GFP (Abcam, ab6556)] were used at 1:1,000 in blocking buffer and de-
413 tected with horseradish peroxidase (HRP)-conjugated secondary antibodies (1:5,000; Ther-
414 moFisher). Membranes were washed in TBST followed by addition of enhanced chemilumines-
415 cent (ECL) reagent (GE Amersham) and visualization using an Azure c300 Darkroom Replacer.

416

417 Protein carbonyl assays

418 Protein carbonyls were quantified using the OxiSelect™ Protein Carbonyl ELISA Kit (Cell
419 Biolabs) following manufacturer's instructions. Briefly, RAW 264.7 cells were seeded at $5x10^5$ in
420 a 6-well plate in DMEM 10% HIFBS. The next day, media were aspirated, and cells were incubated
421 in DMEM/2.5% HIFBS in the presence or absence of 10 μM H_2O_2. After 24 h, cells were washed
422 twice in PBS and lysed in ice-cold 500 μL of detergent-free lysis buffer [25 mM HEPES pH 7.4,
423 150 mM NaCl, 10 mM $MgCl_2$, 1 mM EDTA, 2% glycerol (v/v)] supplemented with complete pro-
424 tease inhibitor cocktail (Roche). Cell lysates were scraped into a pre-chilled microcentrifuge tube
425 and incubated with agitation for 30 min at 4˚C followed by sonication at 40% intensity three times
426 in 10 second intervals. Lysates were clarified by centrifugation at 4˚C for 20 min at 12,000 rpm.
427 Supernatants were transferred to a fresh tube, snap frozen in liquid nitrogen for 2 min and stored
428 at -80˚C until use. Protein concentrations were quantified using a Coomassie Plus (Bradford)
429 Protein Assay (Pierce) and diluted to 10 μg mL^{-1}. Samples and standards were adsorbed to a 96-
430 well protein binding plate and ELISA was performed according to manufacturer's instructions.
431 Absorbance at 450 nm was quantified on a BioTek Epoch2 microplate reader.

432 Protein carbonyls were visualized using the OxiSelect™ Protein Carbonyl Immunoblot Kit
433 (Cell Biolabs). *Tnrf1*$^{-/-}$ BMDMs were seeded in 24-well plates at 2.5x10^5 one day prior to infection
434 with indicated *L. pneumophila* strains at an MOI of 50 in the presence or absence of 10 μM H_2O_2.
435 One hour after infection, cells were washed 3x with PBS$^{-/-}$, media were replaced and cells were
436 incubated for an additional 3 h in the presence or absence of H_2O_2. Cells were washed in ice-cold
437 PBS-/- and lysed in 120 μL ice-cold NP-40 lysis buffer (see above). Lysates were diluted in 3x
438 Laemmli sample buffer and boiled for 10 min. Proteins were separated on a 4-20% gradient SDS-
439 PAGE gel and transferred to PVDF membrane using a BioRad TransBlot semi-dry transfer appa-
440 ratus. Membranes were processed according to manufacturer's instructions using 10 min wash
441 steps. Blots were stripped and re-probed with rabbit α-β-actin antibody (1:1000; Cell Signaling
442 Technology) followed by goat-α-rabbit-HRP (1:5000; ThermoFisher). Blots were visualized as de-
443 scribed above and densitometry was performed using ImageJ.
444
445 Yeast Two-Hybrid Analysis
446 Yeast two-hybrid screening was performed by Hybrigenics Services, S.A.S., Evry, France
447 (http://www.hybrigenics-services.com). The *legC4* coding sequence was PCR-amplified from
448 pSN85::*legC4* (11)and cloned into pB66 as a C-terminal fusion to Gal4 DNA-binding domain
449 (Gal4-C4). The construct was checked by sequencing and used as a bait to screen a random-
450 primed Mouse Spleen library constructed into pP6. pB66 derives from the original pAS2ΔΔ vector
451 (52) and pP6 is based on the pGADGH plasmid (53).
452 60 million clones (6-fold the complexity of the library) were screened using a mating ap-
453 proach with YHGX13 (Y187 ade2-101::loxP-kanMX-loxP, mat-α) and CG1945 (mat-a) yeast
454 strains as previously described (52). 303 His+ colonies were selected on a medium lacking tryp-
455 tophan, leucine and histidine, and supplemented with 2mM 3-aminotriazole to handle bait auto-
456 activation. The prey fragments of the positive clones were amplified by PCR and sequenced at
457 their 5' and 3' junctions. The resulting sequences were used to identify the corresponding

458 interacting proteins in the GenBank database (NCBI) using a fully automated procedure. A confi-
459 dence score (PBS, for Predicted Biological Score) was attributed to each interaction as previously
460 described (54).
461
462 Immunofluorescence Microscopy
463 To quantify LAMP1-LCV co-localization and the number of *L. pneumophila* per LCV, $1x10^5$
464 BMDMs were seeded on poly-L-lysine-coated glass coverslips in 24-well plates and infected with
465 *L. pneumophila* at a multiplicity of infection (MOI) of 30. Coverslips were fixed with 4% para-
466 formaldehyde (PFA; ThermoFisher) and permeabilized in ice cold methanol. Coverslips were
467 stained with 1:1,000 rabbit α-*L. pneumophila* (Invitrogen, PA17227), rat α-LAMP1 (Developmen-
468 tal Studies Hybridoma Bank) primary antibodies and 1:500 Alexa 488-conjugated goat α-rabbit
469 and Alexa594-conjugated goat α-rat secondary antibodies (ThermoFisher) in blocking buffer
470 [0.1% saponin (w/v), 1% HIFBS (v/v), 0.5% bovine serum albumin (BSA; w/v)] in PBS. Nuclei
471 were stained with Hoechst (ThermoFisher) at 1:2,000. Coverslips were mounted on glass slides
472 with ProLong Gold Antifade Mountant (ThermoFisher). Slides were blinded and LAMP1 localiza-
473 tion to LCVs were scored on a Leica DMiL LED inverted epifluorescence microscope (n=150 cells).
474 To image ectopically expressed LegC4 and PA28α, $5x10^5$ HeLa cells were seeded on poly-
475 L-lysine-coated glass coverslips in 24-well tissue culture plates and transfected for 24 h. Co-
476 verslips were fixed in 4% PFA and stained with mouse α-FLAG M2 (1:1,000) and rabbit α-GFP
477 (1:5,000) primary antibodies and 1:5,00 Alexa546-conjugated goat α-mouse and Alexa488-con-
478 jugated goat α-rabbit secondary antibodies, as described above. Images were acquired on a Zeiss
479 AxioPlan LSM-5 laser-scanning confocal microscope (KSU Division of Biology Microscopy Facil-
480 ity). Images were assembled using Fiji-ImageJ and Adobe Photoshop software.
481
482 *L. pneumophila* intracellular growth curves

483 To quantify *L. pneumophila* intracellular replication, macrophages were seeded in 24-well tissue
484 culture plates and infected at an MOI of 1 the next day. BMDMs were seeded at $2.5x10^5$ in seeding
485 media (RPMI, 10% HIFBS, 7.5% L929 cell supernatant), THP-1 cells were seeded at $5x10^5$ and
486 differentiated with 100 nM PMA in RPMI 10% HIFBS for three days. Cells were washed with PBS
487 and incubated in the absence of PMA for one day prior to infection. Stable RAW 264.7 cells were
488 seeded at $2.5x10^5$ in DMEM 2.5%HIFBS. MH-S cells were cultured in RPMI 10% HIFBS and
489 seeded at $2.5x10^5$. At 1 h post-infection, cells were washed 3x with PBS followed by addition of
490 fresh media. Macrophages were lysed in sterile water and colony forming units (CFU) were enu-
491 merated at the indicated time points as described (11). Where indicated, 25 ng mL^{-1} rTNF (Gibco),
492 5 ng mL^{-1} rIFN-γ (Gibco), 10 μM H_2O_2 (VWR), 12.5 nM bafilomycin A1 (BAF; ApexBio), or 100
493 nM ONX 0914 (ApexBio) were added at the time of infection and maintained throughout. DMSO
494 was used as a vehicle control where indicated. Fold replication was quantified by normalizing col-
495 ony forming units to internalized bacteria at 1h post-infection.
496
497 Enzyme-linked immunosorbent assay (ELISA)
498 To quantify TNF secretion, 2.5 x 10^5 BMDMs were seeded in 24-well tissue culture plates and
499 infected with the indicated *L. pneumophila* strains at an MOI of 10. After 1 h of infection, cells
500 were washed with PBS, and media were replaced. Supernatants were at 8 h post-infection and
501 used fresh or stored at -20˚C for up to 1 week and TNF was quantified using mouse TNF-α
502 ELISA MAX kit following manufacturer's instructions. Absorbance at 450 nm was quantified on
503 a BioTek Epoch2 microplate reader.
504
505 Quantification of cell death and metabolic activity
506 To quantify cell death, lactate dehydrogenase activity in cell supernatants was quantified. BMDMs
507 were seeded at $2.5x10^5$ in a 24-well tissue culture plate for 24 h and infected with the indicated *L.*
508 *pneumophila* strains at an MOI of 10 in 500 μL of seeding media (RPMP/10% HIFBS/7.5% L929

509 cell supernatant) and incubated for 10 h. Supernatants were transferred to a 96-well plate and
510 centrifuged at 200 r.c.f. for 10 min. LDH was quantified using the CytoTox 96 Non-Radioactive
511 Cytotoxicity Assay (Promega) according to manufacturer's instructions. Absorbance at 490 nm
512 was quantified on a BioTek Epoch2 microplate reader and percent cytotoxicity was calculated by
513 normalizing absorbance values to cells treated with lysis buffer.

514 To quantify cellular metabolic activity, an MTT colorimetric assay was used. BMDMs were
515 seeded in a 96-well tissue culture plate at $1x10^5$ and infected the next day with the indicated *L.*
516 *pneumophila* strains at an MOI of 10. Cells were treated with 10 ng mL-1 rTNF and/or 10 μM
517 staurosporine (Abcam), as indicated. Cells were assayed using the MTT Cell Proliferation Assay
518 Kit (Colorimetric; BioVision) at 2 h and 24 h post-infection according to manufacturer's instruc-
519 tions. Absorbance at 590 nm was quantified on a BioTek Epoch2 microplate reader and percent
520 viability was calculated by normalizing absorbance values to uninfected cells (100% viability).

521

522 Statistical analysis

523 Statistical analyses were performed with GraphPad Prism 9 software using either Mann-Whitney
524 U test, Students *t*-test, or two-way ANOVA as indicated with a 95% confidence interval. Unless
525 otherwise indicated, data are presented as mean ± standard deviation (s.d.) and statistical analy-
526 sis was performed on samples in triplicates.

527

528 **Acknowledgements**

529 We thank Drs. Philip Hardwidge and Kalyani Pyaram for critical reading of the manuscript and
530 Dr. Mary Weber for assistance with Biorender.com figure preparation. This work was funded by
531 NIH/NIGMS P20GM130448 (to S.R.S.); a Kansas State University Johnson Cancer Research
532 Center Summer Stipend Award (to T.N.); a Kansas-INBRE Postdoctoral Fellowship
533 (P20GM103418 to D.C.); a Kansas-INBRE Semester Scholar Award (P20GM103418 to A.G.S.);
534 and startup funds from Kansas State University (to S.R.S.).

535
536 **REFERENCES**
537

538 1. G. Mitchell, C. Chen, D. A. Portnoy, Strategies Used by Bacteria to Grow in Macrophages. *Mi-*
539 *crobiol Spectr* 4 (2016).

540 2. A. M. Pickering, *et al.*, The immunoproteasome, the 20S proteasome and the PA28αβ pro-
541 teasome regulator are oxidative-stress-adaptive proteolytic complexes. *Biochem J* 432, 585–94
542 (2010).

543 3. I. Dikic, Proteasomal and Autophagy Degradation Systems. *Annu Rev Biochem* 86, 1–32
544 (2016).

545 4. N. de Graaf, *et al.*, PA28 and the proteasome immunosubunits play a central and independent
546 role in the production of MHC class I-binding peptides in vivo. *Eur J Immunol* 41, 926–35
547 (2011).

548 5. T. Preckel, *et al.*, Impaired Immunoproteasome Assembly and Immune Responses in
549 PA28−/− Mice. *Science* 286, 2162–2165 (1999).

550 6. D. Chauhan, S. R. Shames, Pathogenicity and Virulence of *Legionella*: Intracellular replica-
551 tion and host response. *Virulence* 12, 1122–1144 (2021).

552 7. M. F. Fontana, *et al.*, Secreted bacterial effectors that inhibit host protein synthesis are critical
553 for induction of the innate immune response to virulent *Legionella pneumophila*. *Plos Pathog* 7,
554 e1001289 (2011).

555 8. S. Asrat, A. S. Dugan, R. R. Isberg, The frustrated host response to *Legionella pneumophila* is
556 bypassed by MyD88-dependent translation of pro-inflammatory cytokines. *Plos Pathog* 10,
557 e1004229 (2014).

558 9. T. Ngwaga, D. Chauhan, S. R. Shames, Mechanisms of Effector-Mediated Immunity Revealed
559 by the Accidental Human Pathogen *Legionella pneumophila*. *Front Cell Infect Mi* 10, 593823
560 (2021).

561 10. S. R. Shames, *et al.*, Multiple *Legionella pneumophila* effector virulence phenotypes re-
562 vealed through high-throughput analysis of targeted mutant libraries. *Proc National Acad Sci*
563 63, 201708553 (2017).

564 11. T. Ngwaga, A. J. Hydock, S. Ganesan, S. R. Shames, Potentiation of Cytokine-Mediated Re-
565 striction of *Legionella* Intracellular Replication by a Dot/Icm-Translocated Effector. *J Bacteriol*
566 201, 13 (2019).

567 12. A. B. Molofsky, *et al.*, Cytosolic recognition of flagellin by mouse macrophages restricts *Le-*
568 *gionella pneumophila* infection. *J Exp Medicine* 203, 1093 1104 (2006).

569 13. T. Ren, D. S. Zamboni, C. R. Roy, W. F. Dietrich, R. E. Vance, Flagellin-deficient *Legionella*
570 mutants evade caspase-1- and Naip5-mediated macrophage immunity. *Plos Pathog* 2, e18
571 (2006).

572 14. X. Liu, M. A. Boyer, A. M. Holmgren, S. Shin, *Legionella*-Infected Macrophages Engage the
573 Alveolar Epithelium to Metabolically Reprogram Myeloid Cells and Promote Antibacterial In-
574 flammation. *Cell Host Microbe* (2020) https:/doi.org/10.1016/j.chom.2020.07.019.

575 15. U. Seifert, *et al.*, Immunoproteasomes Preserve Protein Homeostasis upon Interferon-In-
576 duced Oxidative Stress. *Cell* 142, 613–624 (2010).

577 16. R. P. Fabunmi, W. C. Wigley, P. J. Thomas, G. N. DeMartino, Interferon gamma regulates
578 accumulation of the proteasome activator PA28 and immunoproteasomes at nuclear PML bod-
579 ies. *J Cell Sci* 114, 29–36 (2001).

580 17. S. Wilk, W.-E. Chen, R. P. Magnusson, Properties of the Beta Subunit of the Proteasome Ac-
581 tivator PA28 (11S REG). *Arch Biochem Biophys* 384, 174–180 (2000).

582 18. J. D. Mott, *et al.*, PA28, an activator of the 20 S proteasome, is composed of two nonidentical
583 but homologous subunits. *J Biological Chem* 269, 31466–71 (1994).

584 19. K. Hallermalm, *et al.*, Tumor necrosis factor-α induces coordinated changes in major histo-
585 compatibility class I presentation pathway, resulting in increased stability of class I complexes at
586 the cell surface. *Blood* 98, 1108–1115 (2001).

587 20. J. Li, S. R. Powell, X. Wang, Enhancement of proteasome function by PA28α; overexpres-
588 sion protects against oxidative stress. *Faseb J* 25, 883–93 (2010).

589 21. S. M. Rabadi, *et al.*, Antioxidant Defenses of *Francisella tularensis* Modulate Macrophage
590 Function and Production of Proinflammatory Cytokines. *J Biological Chem* 291, 5009–21
591 (2015).

592 22. P. Bandyopadhyay, B. Byrne, Y. Chan, M. S. Swanson, H. M. Steinman, *Legionella pneu-*
593 *mophila* Catalase-Peroxidases Are Required for Proper Trafficking and Growth in Primary Mac-
594 rophages. *Infect Immun* 71, 4526–4535 (2003).

595 23. H.-K. An, *et al.*, CASP9 (caspase 9) is essential for autophagosome maturation through regu-
596 lation of mitochondrial homeostasis. *Autophagy* 16, 1–20 (2019).

597 24. T. Harada, M. Miyake, Y. Imai, Evasion of *Legionella pneumophila* from the Bactericidal
598 System by Reactive Oxygen Species (ROS) in Macrophages. *Microbiol Immunol* 51, 1161–1170
599 (2007).

600 25. K. J. Flynn, M. S. Swanson, Integrative Conjugative Element ICE-βox Confers Oxidative
601 Stress Resistance to *Legionella pneumophila* In Vitro and in Macrophages. *Mbio* 5, e01091-14
602 (2014).

603 26. P. Bandyopadhyay, H. M. Steinman, Catalase-Peroxidases of *Legionella pneumophila*: Clon-
604 ing of the katA Gene and Studies of KatA Function. *J Bacteriol* 182, 6679–6686 (2000).

605 27. U. B. Pandey, *et al.*, HDAC6 rescues neurodegeneration and provides an essential link be-
606 tween autophagy and the UPS. *Nature* 447, 860–864 (2007).

607 28. C. R. Roy, K. H. Berger, R. R. Isberg, *Legionella pneumophila* DotA protein is required for
608 early phagosome trafficking decisions that occur within minutes of bacterial uptake. *Mol Micro-*
609 *biol* 28, 663–674 (1998).

610 29. M. S. Swanson, R. R. Isberg, Association of *Legionella pneumophila* with the macrophage
611 endoplasmic reticulum. *Infection and immunity* 63, 3609 3620 (1995).

612 30. N. Matsumoto, M. Nakanishi-Matsui, Proton pumping V-ATPase inhibitor bafilomycin A1
613 affects Rab7 lysosomal localization and abolishes anterograde trafficking of osteoclast secretory
614 lysosomes. *Biochem Bioph Res Co* 510, 421–426 (2019).

615 31. S. Sturgill-Koszycki, M. S. Swanson, *Legionella pneumophila* Replication Vacuoles Mature
616 into Acidic, Endocytic Organelles. *J Exp Medicine* 192, 1261–1272 (2000).

617 32. A. A. Khweek, *et al.*, A bacterial protein promotes the recognition of the *Legionella pneu-*
618 *mophila* vacuole by autophagy. *Eur J Immunol* 43, 1333 1344 (2013).

619 33. S. C. Xie, *et al.*, The structure of the PA28-20S proteasome complex from *Plasmodium falci-*
620 *parum* and implications for proteostasis. *Nat Microbiol* 4, 1990–2000 (2019).

621 34. J. Lesne, *et al.*, Conformational maps of human 20S proteasomes reveal PA28- and im-
622 muno-dependent inter-ring crosstalks. *Nat Commun* 11, 6140 (2020).

623 35. C. T. D. Price, *et al.*, Dot/Icm-Dependent Restriction of *Legionella pneumophila* within Neu-
624 trophils. *Mbio* 12, e01008-21 (2021).

625 36. P. Ziltener, T. Reinheckel, A. Oxenius, Neutrophil and Alveolar Macrophage-Mediated In-
626 nate Immune Control of *Legionella pneumophila* Lung Infection via TNF and ROS. *Plos Pathog*
627 12, e1005591 (2016).

628 37. J. D. MacMicking, Interferon-inducible effector mechanisms in cell-autonomous immunity.
629 *Nat Rev Immunol* 12, 367 382 (2012).

630 38. J. Naujoks, *et al.*, IFNs Modify the Proteome of *Legionella*-Containing Vacuoles and Restrict
631 Infection Via IRG1-Derived Itaconic Acid. *Plos Pathog* 12, e1005408 (2016).

632 39. A. Orvedahl, *et al.*, Autophagy genes in myeloid cells counteract IFNγ-induced TNF-medi-
633 ated cell death and fatal TNF-induced shock. *Proc National Acad Sci* 116, 16497–16506 (2019).

634 40. B. G. Byrne, J.-F. Dubuisson, A. D. Joshi, J. J. Persson, M. S. Swanson, Inflammasome Com-
635 ponents Coordinate Autophagy and Pyroptosis as Macrophage Responses to Infection. *Mbio* 4,
636 e00620-12 (2013).

637 41. J. N. Shin, E. A. Fattah, A. Bhattacharya, S. Ko, N. T. Eissa, Inflammasome Activation by Al-
638 tered Proteostasis*. *J Biol Chem* 288, 35886–35895 (2013).

639 42. A. Marra, S. J. Blander, M. A. Horwitz, H. A. Shuman, Identification of a *Legionella pneu-*
640 *mophila* locus required for intracellular multiplication in human macrophages. *Proc Natl Acad*
641 *Sci* 89, 9607–9611 (1992).

642 43. J. Zhao, *et al.*, Molecular basis for the binding and modulation of V-ATPase by a bacterial
643 effector protein. *Plos Pathog* 13, e1006394 (2017).

644 44. A. Choy, *et al.*, The *Legionella* effector RavZ inhibits host autophagy through irreversible
645 Atg8 deconjugation. *Science* 338, 1072 1076 (2012).

646 45. M. Rolando, *et al.*, *Legionella pneumophila* S1P-lyase targets host sphingolipid metabolism
647 and restrains autophagy. *Proc Natl Acad Sci* 113, 1901 1906 (2016).

648 46. M. Rolando, P. Escoll, C. Buchrieser, *Legionella pneumophila* restrains autophagy by modu-
649 lating the host's sphingolipid metabolism. *Autophagy* 12, 1053–1054 (2016).

650 47. J. C. Feeley, *et al.*, Charcoal-yeast extract agar: primary isolation medium for *Legionella*
651 *pneumophila*. *J Clin Microbiol* 10, 437 441 (1979).

652 48. A. Saito, R. D. Rolfe, P. H. Edelstein, S. M. Finegold, Comparison of liquid growth media for
653 *Legionella pneumophila*. *J Clin Microbiol* 14, 623 627 (1981).

654 49. C. L. Case, C. R. Roy, Analyzing caspase-1 activation during *Legionella pneumophila* infec-
655 tion in macrophages. *Methods Mol Biol (Clifton, NJ)* 954, 479 491 (2013).

656 50. A. Ingmundson, A. Delprato, D. G. Lambright, C. R. Roy, *Legionella pneumophila* proteins
657 that regulate Rab1 membrane cycling. *Nature* 450, 365–369 (2007).

658 51. S. R. Shames, *et al.*, The pathogenic *E. coli* type III effector EspZ interacts with host CD98
659 and facilitates host cell prosurvival signalling. *Cell Microbiol* 12, 1322 1339 (2010).

660 52. M. Fromont-Racine, J.-C. Rain, P. Legrain, Toward a functional analysis of the yeast genome
661 through exhaustive two-hybrid screens. *Nat Genet* 16, 277–282 (1997).

662 53. P. L. Bartel, S. Fields, [16] Analyzing protein-protein interactions using two-hybrid system.
663 *Methods Enzymol* 254, 241–263 (1995).

664 54. E. Formstecher, *et al.*, Protein interaction mapping: A *Drosophila* case study. *Genome Res*
665 15, 376–384 (2005).

666

667

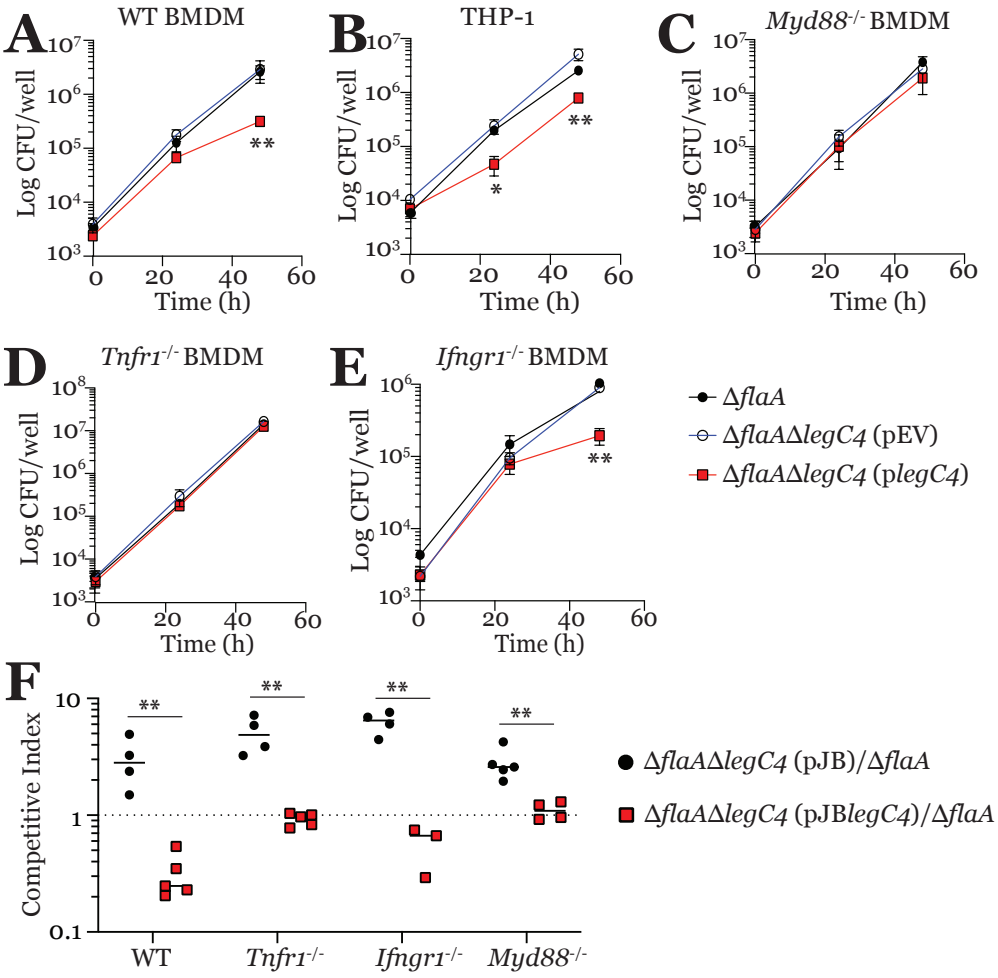

Figure 1. LegC4 attenuates *L. pneumophila* replication within cytokine-activated macrophages and the mouse lung. Growth of indicated *L. pneumophila* strains within **(A)** WT BMDMs, **(B)** THP-1 cells, **(C)** *Myd88*$^{-/-}$ BMDMs, **(D)** *Tnfr1*$^{-/-}$ BMDMs, or **(E)** *Ifngr1*$^{-/-}$ BMDMs over 48 h. Plasmid expression of *legC4* was induced with 1 mM IPTG. Macrophages were infected in triplicates and data are presented as mean ± standard deviation (s.d.). Asterisks denote statistical significance by Student's *t*-test (**P*<0.05, ***P*<0.01). **(F)** Competitive index (CI) of *L. pneumophila* Δ*flaA*Δ*legC4* (pJB*legC4*) or Δ*flaA*Δ*legC4* (pJB) versus *L. pneumophila* Δ*flaA* in the lungs of the indicated mice at 48 h post-infection. Each symbol represents an individual animal and asterisks denote statistical significance by Mann-Whitney U test (***P*<0.01). Data shown are representative of at least three independent experiments.

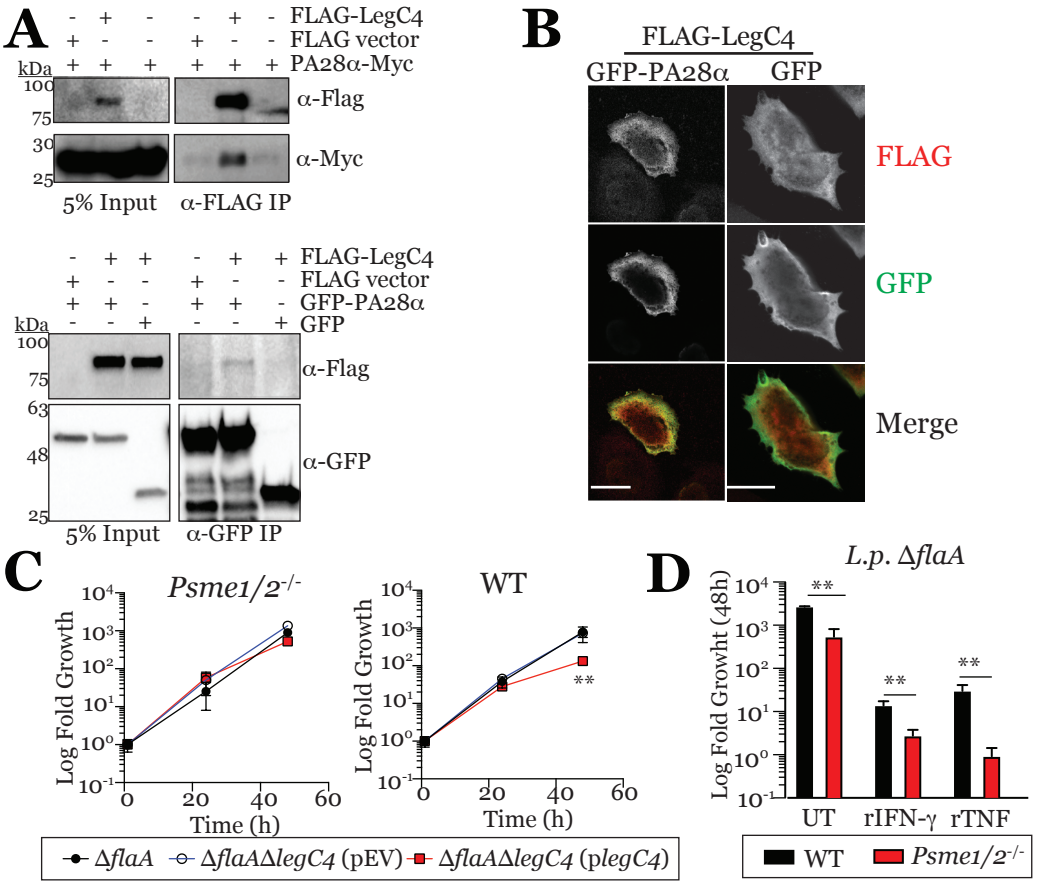

Figure 2. LegC4 binds and functions through PA28αβ. **(A)** Western blot of co-immunoprecipitation of PA28α-Myc with 3xFLAG-LegC4 on α-FLAG conjugated magnetic beads (top) or 3xFLAG-LegC4 with GFP-PA28α on α-GFP-conjugated magnetic beads (bottom) from lysates of transfected HEK 293T cells. **(B)** Confocal microscopy to image HeLa cells co-transfected to ectopically produce 3xFLAG-LegC4 (red) and either GFP-PA28α or GFP (green). Scale bar represents 10 µm. **(C)** Fold replication of indicated *L. pneumophila* strains within *Psme1/2*$^{-/-}$ (left) or WT (right) BMDMs. Plasmid expression of *legC4* was induced with 1 mM IPTG. **(D)** Fold replication of *L. pneumophila* (*L.p.*) Δ*flaA* within WT or *Psme1/2*$^{-/-}$ BMDMs at 48 h post-infection. Where indicated BMDMs were treated with 25 ng mL^{-1} recombinant mouse (r)TNF, 5 ng mL^{-1} rIFN-γ, or left untreated (UT). Macrophages were infected in triplicates and data are presented as

691 mean ± s.d. Asterisks denote statistical significance (**P<0.01) by Students' t-test. Data shown

692 are representative of at least two independent experiments.

693

694

695

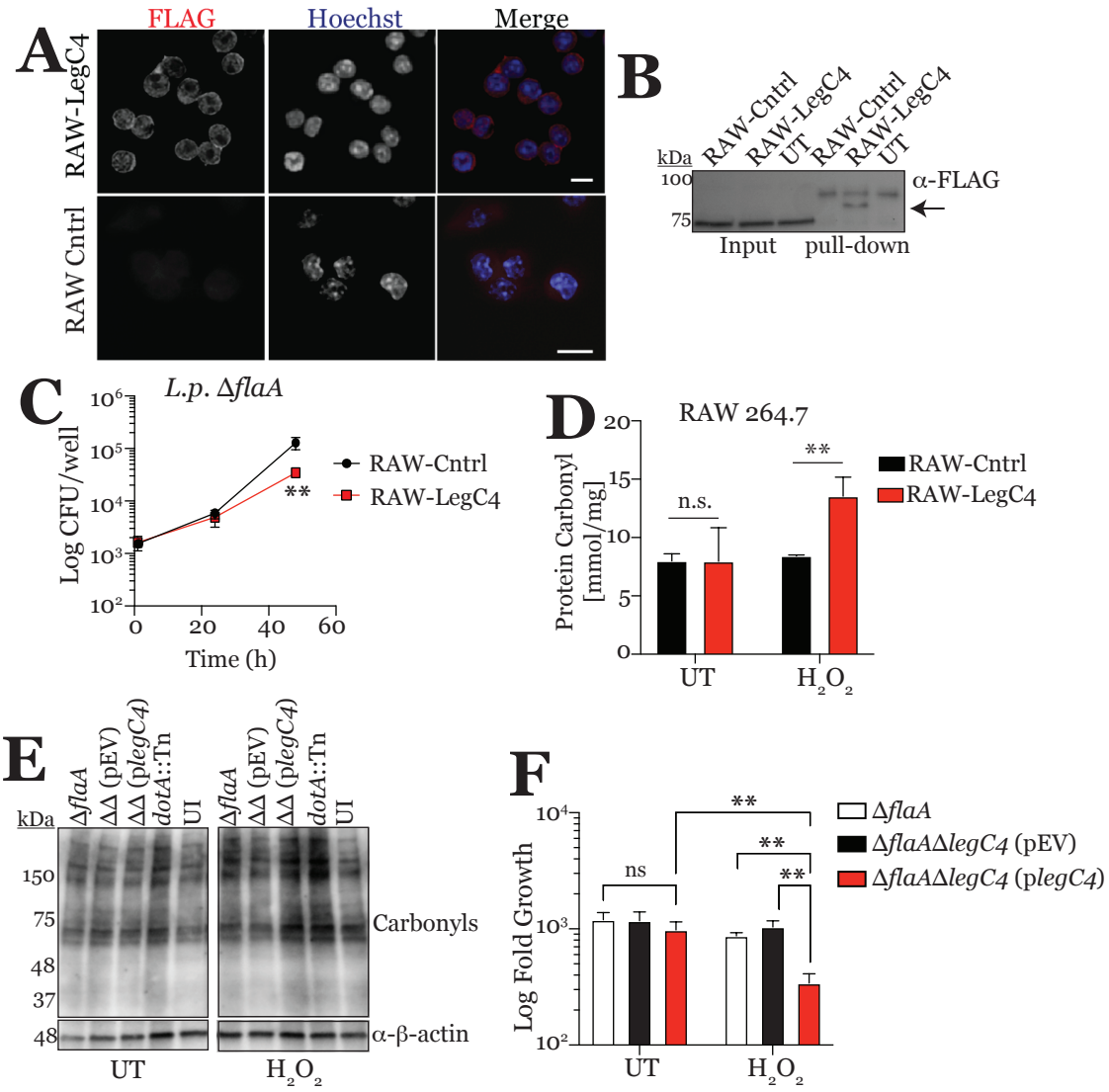

696

697 **Figure 3.** LegC4 impairs resolution of oxidative stress, which is sufficient for *L. pneumophila*
698 restriction. **(A)** Confocal microscopy to visualize 3xFLAG-LegC4 (red) production by stable RAW
699 264.7 cells (RAW-LegC4). Mock transfected cells (RAW-Cntrl) were used as a control and nuclei
700 were imaged with Hoechst. Scale bar represents 10 μm. **(B)** Western blot analysis of 3xFLAG-
701 LegC4 immunoprecipitated from lysates of RAW-LegC4, RAW-Cntrl or untransfected (UT) RAW
702 cells using α-FLAG-conjugated beads. Arrow indicates 3xFLAG-LegC4 (~84 kDa). **(C)** Growth of
703 *L. pneumophila ΔflaA* within RAW-LegC4 and -Cntrl cells infected for up to 48 h. **(D)** ELISA

704 quantification of protein carbonyls in lysates of RAW-LegC4 and -Cntrl cells incubated for 24 h
705 in the presence or absence of 10 μM H_2O_2. **(E)** Western blot for protein carbonyls and actin (load-
706 ing control) in lysates of *Tnfr1*$^{-/-}$ BMDMs infected for 4 h with the indicated strains. ΔΔ:
707 Δ*flaA*Δ*legC4*; plasmid expression of *legC4* was induced with 1 mM IPTG. **(F)** Fold replication of
708 *L. pneumophila* strains at 48 h post-infection within *Tnfr1*$^{-/-}$ BMDMs in the presence or absence
709 of 10 μM H_2O_2 as indicated. Plasmid expression of *legC4* was induced with 1 mM IPTG. All quan-
710 titative data are presented as mean ± s.d. from samples in triplicates and are representative of at
711 least two independent experiments. Asterisks denote statistical significance by Students' *t*-test
712 (**P<0.01; n.s., not significant).
713

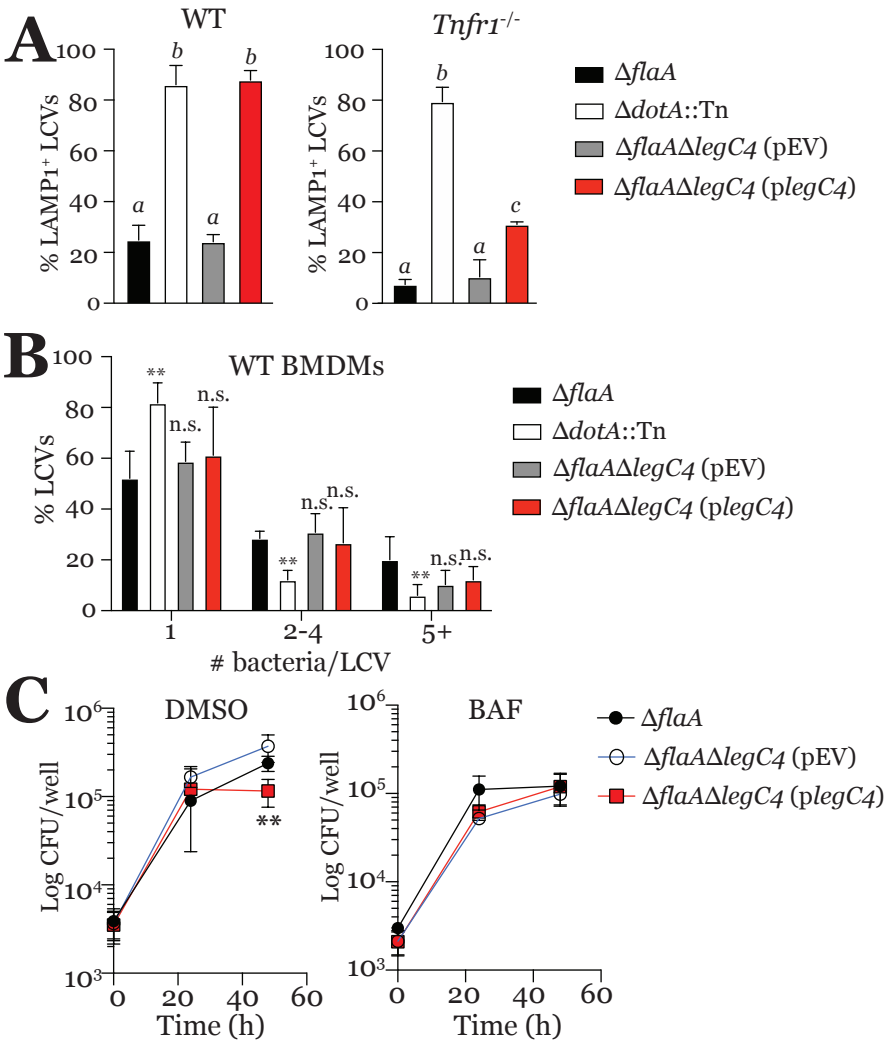

714

715 **Figure 4**. Role of phagolysosomal fusion in LegC4-mediated restriction of *L. pneumophila*. **(A)**
716 Blinded immunofluorescence scoring of LAMP1 localization to LCVs within WT or *Tnfr1*$^{-/-}$
717 BMDMs after 9 h of infection. Plasmid expression of *legC4* was induced with 1 mM IPTG. Data
718 are representative of at least two independent experiments ($n \geq 150$ per experiment) and letters
719 denote statistical significance by Students' *t*-test ($P<0.05$). letters not significant) of values com-
720 pared to Δ*flaA*. **(B)** WT BMDMs were infected with the indicated *L. pneumophila* strains and the
721 number of bacteria per LCV was quantified by blinded immunofluorescence scoring. Data are
722 representative of at least two independent experiments ($n \geq 150$ per experiment) and asterisks
723 denote statistical significance by Students' *t*-test (**$P<0.01$; n.s., not significant) of values com-
724 pared to Δ*flaA*. Plasmid expression of *legC4* was induced with 1 mM IPTG. **(C)** Growth of

725 indicated *L. pneumophila* strains within WT BMDMs treated with 12.5 nM bafilomycin A1 (BAF)
726 or DMSO (vehicle control). Plasmid expression of *legC4* was induced with 1 mM IPTG. Data are
727 presented as mean ± s.d. of samples in triplicates and are representative of at least two independ-
728 ent experiments. Asterisks denote statistical significance by Students' *t*-test ($^{**}P<0.01$).
729